

УДК 517.977 + 519.63

CONTROL DESIGN IN CRYOPRESERVATION OF LIVING CELLS¹**N. D. Botkin, K.-H. Hoffmann**

A mathematical model of ice formation in living cells during freezing is considered. Application of an appropriate averaging technique to partial differential equations describing the dynamics of water-ice phase transitions reduces spatially distributed relations to a few ordinary differential equations with control parameters and uncertainties. Such equations together with an objective functional that expresses the difference between the amount of ice inside and outside of a cell are considered as a differential game where the aim of the control is to minimize the objective functional, and the aim of the disturbance is opposite. A stable finite-difference scheme for computing the value function is presented. Based on the computed value function, optimal controls are designed to produce cooling protocols ensuring simultaneous freezing of water inside and outside of living cells. Such a regime provides balancing the pressures inside and outside of cells, which prevents cells from injuring.

Key words: cryopreservation, cooling rate, optimal control, differential game, value function, finite-difference scheme.

Introduction

Numerous modern medical technologies involve freezing and thawing small tissue samples in such a manner that the cells preserve their functional properties. Optimization and control are necessary here to improve the viability of cells by reducing injuring factors. The main of them is a large stress exerted on cell membranes and occurring at slow cooling because of non-simultaneous freezing of extracellular and intracellular fluids. The use of rapid cooling rates is not a perfect solution because water inside cells forms small, irregularly-shaped ice crystals (dendrites) that are relatively unstable. If frozen cells are subsequently thawed out, dendrites will aggregate to form larger, more stable crystals that may cause damage.

The objective of this work is to apply control theory to provide simultaneous freezing of extracellular and intracellular fluids even for slow cooling rates. Therefore, a mathematical model describing freezing and thawing, along with optimization criteria, is to be formulated. Note that models of phase transitions are basically utilize partial differential equations that describe the dynamics of phases in each spatial point (see e.g. [3, 6, 7]). Nevertheless, the spatial distribution is not very important, if small objects such as living cells and pores of the extracellular matrix are investigated. Our experience shows that appropriate averaging techniques accurately reduce spatially distributed models to a few ordinary differential equations with control parameters and uncertainties. However, such equations contain as a rule nonlinear dependencies given by tabular data. Thus, the uncertainties and non-smooth nonlinearities complicate the application of traditional control design methods based on Pontryagin's maximum principle. Nevertheless, the dynamical programming principle related to Hamilton—Jacobi—Bellman—Isaacs (HJBI) equations is suitable, if stable grid methods for solving HJBI are available. This paper considers a stable grid procedure that allows us to design optimized controls (cooling protocols) in a differential game describing competitive ice formation inside and outside of living cells.

¹The work is supported by the German Research Society (DFG), Project SPP 1253

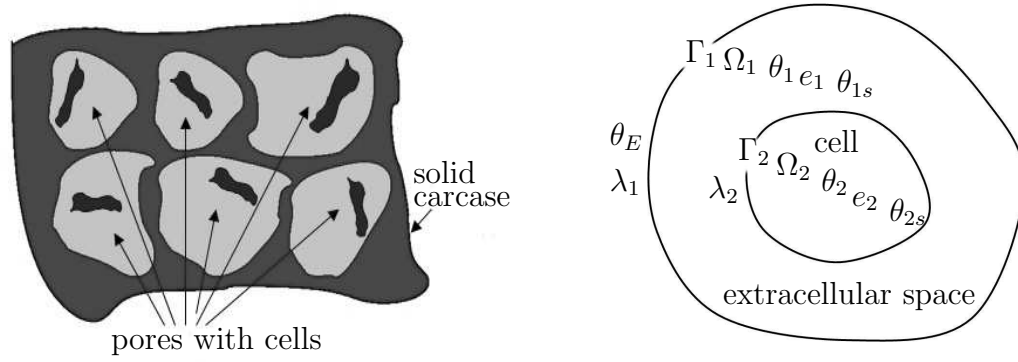


Fig 1. Two-dimensional sketch of the extracellular matrix with pores containing an extracellular fluid and living cells filled by an intracellular liquid (to the left). Schematic notation of variables and three-dimensional regions when considering a single pore (to the right). Note that Γ_1 and Γ_2 are the boundaries of the pore and the cell, respectively, Ω_1 is the region lying between Γ_1 and Γ_2 (extracellular space), and Ω_2 is the region of the cell.

1. Mathematical model of ice formation

Remember that cells of a tissue are located in pores of an extracellular matrix (see a sketch in the left part of Fig. 1). Each pore is filled by a solution called extracellular liquid and contains a cell. The extracellular fluid freezes earlier than the intracellular one, and the volumetric increase of ice produces a great pressure exerted on cells. The magnitude of the effect can be approximately estimated as $p \approx C^{\text{ice}} \cdot \alpha \cdot (1 - \beta_\ell)$, where p is the pressure, C^{ice} is the elasticity of ice, α is the expansion coefficient of ice, β_ℓ is the unfrozen water fraction. A rough estimate yields: $p \approx 1\text{Bar}$, which is totally injuring for cell membranes. The conventional method to avoid that is lowering the freezing point of the extracellular liquid to give a chance the extracellular and intracellular fluids to be frozen simultaneously. Then, a proper cooling protocol is to be adjusted experimentally. Our objective is to develop numerical techniques for the design of such protocols.

In the case were a fluid fills a micro volume, say $\Omega \in \mathbb{R}^3$, bounded by a solid wall, the unfrozen water fraction β_ℓ can be computed using the following phase field model (see [6]):

$$\begin{aligned} \frac{\partial e(\theta)}{\partial t} - \mathcal{K} \Delta \theta &= 0, & -\mathcal{K} \frac{\partial \theta}{\partial \nu} \Big|_{\partial \Omega} &= \lambda (\theta - \theta_{\text{ext}}) \Big|_{\partial \Omega}, \\ e(\theta) &= \rho \mathcal{C} \theta + \rho L \beta_\ell(\theta), & \beta_\ell(\theta) &= \phi \left(\frac{L(\theta - \theta_s)}{(T_0 + \theta_s)(T_0 + \theta)} \right), \end{aligned} \quad (1.1)$$

where θ is the Celsius temperature, \mathcal{K} the heat conductivity coefficient, λ the overall (film) heat transfer coefficient, θ_{ext} the temperature outside the region where model (1.1) is considered, i.e. the temperature behind the boundary film, \mathcal{C} the specific heat capacity, ρ the density, L the latent heat, θ_s the freezing (solidification) point, T_0 the Celsius zero point (273°K). The function $e(\theta)$ has the sense of the internal energy. The function ϕ is recovered from experimental data.

Consider now a sketch of a pore shown in Fig. 1 (to the right). The notations are self-explanatory. It is only to note that λ_1 and λ_2 denote the film heat transfer coefficients of the pore boundary and the cell membrane, respectively; θ_{1s} and θ_{2s} stand for the freezing points of the extracellular and intracellular liquids, respectively. Integrating the energy balance equation of (1.1) over Ω_1 and Ω_2 , using the following notations for mean values:

$$\hat{e}_i = \frac{1}{|\Omega_i|} \int_{\Omega_i} e_i dV, \quad \hat{\theta}_i = \frac{1}{|\Gamma_i|} \int_{\Gamma_i} \theta_i dS, \quad \hat{\theta}_E = \frac{1}{|\Gamma_1|} \int_{\Gamma_1} \theta_E dS, \quad \hat{\alpha}_i = \frac{|\Gamma_2|}{|\Omega_i|} \lambda_2, \quad \hat{\lambda} = \frac{|\Gamma_1|}{|\Omega_1|} \lambda_1,$$

and assuming that $|\Gamma_1|^{-1} \int_{\Gamma_1} \theta_1 dS \approx |\Gamma_2|^{-1} \int_{\Gamma_2} \theta_1 dS$ because θ_1 is almost constant in the small region Ω_1 , yield the following coupled system of ordinary differential equations:

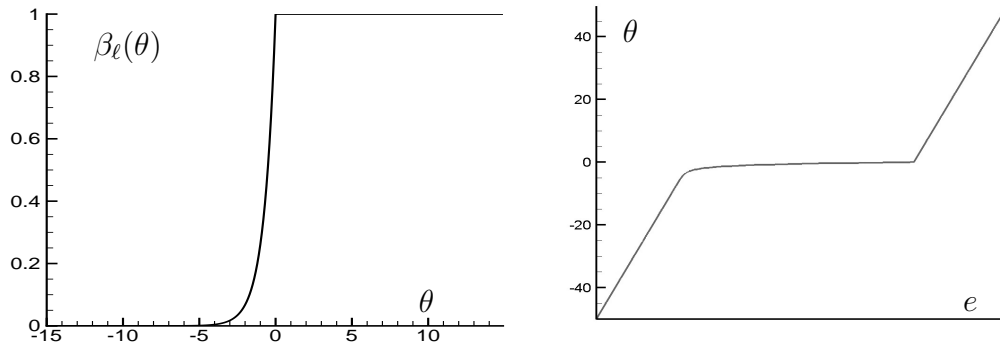


Fig 2. Dependence of the unfrozen water fraction on the temperature (to the left). Graph of the inverse function to $e(\theta)$ (to the right).

$$\frac{d}{dt}\hat{e}_1 = -\hat{\alpha}_1[\hat{\theta}_1 - \hat{\theta}_2] - \hat{\lambda}[\hat{\theta}_1 - \hat{\theta}_E], \quad \frac{d}{dt}\hat{e}_2 = -\hat{\alpha}_2[\hat{\theta}_2 - \hat{\theta}_1]. \quad (1.2)$$

The relation between \hat{e}_i and $\hat{\theta}_i$ (see (1.1)) is given by the formula

$$\hat{e}_i = \rho C \hat{\theta}_i + \rho L \beta_\ell^i(\hat{\theta}_i), \quad (1.3)$$

where β_ℓ^1 and β_ℓ^2 are defined by the replacement of θ_s with θ_{1s} and θ_{2s} , respectively, in (1.1).

Note that the derivatives $\partial \hat{e}_i / \partial \hat{\theta}_i$, $i = 1, 2$, are discontinuous (see equation (1.3) and the left graph of Fig. 2). Therefore, the direct form of equations (1.2) is not appropriate. It is convenient to express the temperatures $\hat{\theta}_1$ and $\hat{\theta}_2$ through the energies \hat{e}_1 and \hat{e}_2 , respectively, using the relation $\hat{\theta}_i = \Theta_i(\hat{e}_i)$ which is the inverse of relation (1.3) (see the right graph of Fig. 2). By doing that, we obtain the following system of ordinary differential equations:

$$\dot{\hat{e}}_1 = -\hat{\alpha}_1[\Theta_1(\hat{e}_1) - \Theta_2(\hat{e}_2)] - \hat{\lambda}[\Theta_1(\hat{e}_1) - \hat{\theta}_E], \quad \dot{\hat{e}}_2 = -\hat{\alpha}_2[\Theta_2(\hat{e}_2) - \Theta_1(\hat{e}_1)].$$

For simplicity, denote $x = \hat{e}_1$, $y = \hat{e}_2$, $z = \hat{\theta}_E$, $\alpha_i = \hat{\alpha}_i$, $\lambda = \hat{\lambda}$ and consider the following controlled system:

$$\begin{aligned} \dot{x} &= -\alpha_1[\Theta_1(x) - \Theta_2(y)] - \lambda[\Theta_1(x) - z] - d + v_1 & (= f_1), \\ \dot{y} &= -\alpha_2[\Theta_2(y) - \Theta_1(x)] + v_2 & (= f_2), \\ \dot{z} &= u & (= f_3). \end{aligned} \quad (1.4)$$

Here, z is the temperature outside of the pore (chamber temperature), u is the cooling rate, v_1 , v_2 are errors in data interpreted as disturbances. The control u is restricted as $|u| \leq \mu$, the disturbances v_1 , v_2 as $|v_1| \leq \nu$, $|v_2| \leq \nu$. Since the zero initial value for z is always assumed, the constant d is introduced to emulate nonzero initial values of z (the initial chamber temperatures).

The definition of the function β_ℓ says that exact simultaneous freezing of the extracellular and intracellular liquids can be expressed as the vanishing of the following functional:

$$J = \max_{t \in [0, t_f]} \gamma(x(t), y(t)), \quad (1.5)$$

where

$$\gamma(x, y) = |\beta_\ell^1(\Theta_1(x)) - \beta_\ell^2(\Theta_2(y))|$$

estimates the difference of the ice fractions in the extra- and intracellular regions.

Consider differential game (1.4), (1.5) where the objective of the control u is to minimize the functional J , whereas the objective of the disturbance is opposite. The differential game will be solved numerically using approximation schemes described below. The value function is being computed as a viscosity solution to an appropriate HJBI equation, and the optimal feedback control is being designed by applying the procedure of extremal aiming [9, 10].

2. Hamilton—Jacobi—Bellman—Isaacs equations

The game (1.4), (1.5) is formalized as in [9, 10, 13] so that the value function V exists. The next important result proved in [14] says that V coincides with a unique viscosity solution (see [1, 4, 5]) of the following HJBI equation:

$$V_t + H(x, y, z, V_x, V_y, V_z) = 0, \quad (2.1)$$

where the Hamiltonian H and the terminal condition are defined as

$$H(x, y, z, p_1, p_2, p_3) = \max_{|v_1|, |v_2| \leq \nu} \min_{|u| \leq \mu} \sum_{i=1}^3 p_i f_i, \quad V(t_f, x, y, z) = \gamma(x, y).$$

In the next section, an approximation scheme for solving this HJBI equation is discussed and convergence results are given.

3. Approximation schemes and convergence results

Let $\tau, \Delta_x, \Delta_y, \Delta_z$ be time and space discretization step sizes. Introduce the following notation:

$$V^n(x_i, y_j, z_k) = V(n\tau, i\Delta_x, j\Delta_y, k\Delta_z), \quad V^{\mathcal{N}} = V(t_f)$$

and consider a difference scheme:

$$V^{n-1}(x_i, y_j, z_k) = V^n(x_i, y_j, z_k) + \tau H(x_i, y_j, z_k, V_x^n, V_y^n, V_z^n), \quad V^{\mathcal{N}}(x_i, y_j, z_k) = \gamma(x_i, y_j).$$

Here, the symbols V_x^n, V_y^n, V_z^n denote finite difference approximations (left, right, central and etc.) of the corresponding partial derivatives. The scheme can be considered as the application of an operator Π to the grid function V^n to obtain V^{n-1} :

$$V^{n-1} = \Pi(V^n; \tau, \Delta_x, \Delta_y, \Delta_z).$$

It is clear that such an operator can be naturally extended to continuum functions.

Definition 1. The operator Π is monotone, if the following implication holds:

$$V \leq W \Rightarrow \Pi(V; \tau, \Delta_x, \Delta_y, \Delta_z) \leq \Pi(W; \tau, \Delta_x, \Delta_y, \Delta_z),$$

where the point-wise order is assumed.

Definition 2. The operator Π has the generator property, if the following estimate holds:

$$\left| \frac{\Pi(\phi; \tau, a\tau, b\tau, c\tau)(\vec{r}) - \phi(\vec{r})}{\tau} - H(\vec{r}, D\phi(\vec{r})) \right| \leq C(1 + \|D\phi\| + \|D^2\phi\|)\tau \quad (3.1)$$

for every $\phi \in C_b^2(\mathbb{R}^3)$, $\vec{r} = (x, y, z) \in \mathbb{R}^3$, and fixed $a, b, c > 0$. Here $C_b^2(\mathbb{R}^3)$ is the space of twice continuously differentiable functions defined on \mathbb{R}^3 and bounded together with their two derivatives, $\|\cdot\|$ denotes the point-wise maximum norm, $D\phi$ and $D^2\phi$ denote the gradient and the Hessian matrix of ϕ .

Theorem 1. (convergence, [1, 12]). Assume that the operator $\Pi(\cdot; \tau, a\tau, b\tau, c\tau)$ is monotone for any $\tau > 0$ and satisfies the generator property, then the grid function obtained by the procedure:

$$V^{n-1} = \max\{\Pi(V^n; \tau, a\tau, b\tau, c\tau), \gamma\}, \quad V^{\mathcal{N}} = \gamma,$$

converges point-wise to a unique viscosity solution of (2.1) and, therefore, to the value function of the differential game (1.4), (1.5) as $\tau \rightarrow 0$. The convergence rate is $\sqrt{\tau}$.

Remark 1. Theorem 1 refer only to the monotonicity and generator properties of the operator Π . Really, some secondary properties must be held to provide the convergence (see [1, 12]). We omit here the discussion of them because they obviously hold for an operator Π that will be considered further.

The next section presents an upwind operator Π with the monotonicity and generator properties. Denote

$$\begin{aligned} p_1^R &= [V^n(x_{i+1}, y_j, z_k) - V^n(x_i, y_j, z_k)]/\Delta_x, & p_1^L &= [V^n(x_i, y_j, z_k) - V^n(x_{i-1}, y_j, z_k)]/\Delta_x, \\ p_2^R &= [V^n(x_i, y_{j+1}, z_k) - V^n(x_i, y_j, z_k)]/\Delta_y, & p_2^L &= [V^n(x_i, y_j, z_k) - V^n(x_i, y_{j-1}, z_k)]/\Delta_y, \\ p_3^R &= [V^n(x_i, y_j, z_{k+1}) - V^n(x_i, y_j, z_k)]/\Delta_z, & p_3^L &= [V^n(x_i, y_j, z_k) - V^n(x_i, y_j, z_{k-1})]/\Delta_z. \end{aligned}$$

4. Upwind solution operator

We will consider a solution operator proposed in [11] and prove that it is monotone and possesses the generator property, which proves convergence claims. Unfortunately, the convergence arguments given in [11] are very sketchy and not strong. They are solely based on topological considerations and do not take into account the nature of viscosity solutions so that they have little force. Nevertheless, the idea of the operator proposed there is brilliant.

Assume that the right-hand-sides f_i , $i = 1, 2, 3$, are now arbitrary functions of the state (x, y, z) , control $u \in P \subset \mathbb{R}^p$, and disturbance $v \in Q \subset \mathbb{R}^q$. Denote $a^+ = \max(a, 0)$, $a^- = \min(a, 0)$. The operator introduced in [11] assumes the following approximations of the spatial derivatives:

$$V_x^n \cdot f_1 = p_1^R \cdot f_1^+ + p_1^L \cdot f_1^-, \quad V_y^n \cdot f_2 = p_2^R \cdot f_2^+ + p_2^L \cdot f_2^-, \quad V_z^n \cdot f_3 = p_3^R \cdot f_3^+ + p_3^L \cdot f_3^-,$$

where f_1, f_2, f_3 are computed at (x_i, y_j, z_k) ; p_1^R, p_2^R, p_3^R and p_1^L, p_2^L, p_3^L the right and left divided differences, respectively. Finally, the operator is given by

$$\begin{aligned} \Pi(V^n; \tau, \Delta_x, \Delta_y, \Delta_z)(x_i, y_j, z_k) &= V^n(x_i, y_j, z_k) \\ &+ \tau \max_{v \in Q} \min_{u \in P} (p_1^R \cdot f_1^+ + p_1^L \cdot f_1^- + p_2^R \cdot f_2^+ + p_2^L \cdot f_2^- + p_3^R \cdot f_3^+ + p_3^L \cdot f_3^-). \end{aligned} \quad (4.1)$$

Lemma 1 (monotonicity and generator property, [2]). *Let M be the bound of the right hand side of the controlled system. If $a, b, c \geq M\sqrt{3}$, then the operator $\Pi(\cdot; \tau, a\tau, b\tau, c\tau)$ given by (4.1) is monotone. The generator property (3.1) holds for any fixed a, b, c .*

Thus, the operator (4.1) satisfies the conditions of Theorem 1.

Remark 2. If the functions f_i , $i = 1, 2, 3$, are linear in u and v at each fixed state (x, y, z) , then the operation $\max_{v \in Q} \min_{u \in P}$ in the definitions of the operator (4.1) can be replaced by $\max_{v \in \text{ext } Q} \min_{u \in \text{ext } P}$, where “ext” returns the set of the extremal points. In particular, “max min” can be computed over the set of vertices, if P and Q are polyhedrons. The monotonicity holds independently of the structure of the sets P and Q . To prove the generator property, it is sufficient to observe that the Hamiltonian is equal to that computed using the sets $\text{ext } P$ and $\text{ext } Q$ whenever the assumptions of linearity in u and v at each fixed state vector holds. Note that this remark is very important for numerical implementations of the operator (4.1) because the operation “max min” is applied to a function that is nonlinear and not convex/concave in u and v .

5. Control procedure

In this section, the computation of optimal controls for system (1.4) in accordance with the procedure of extremal aiming (see [9, 10]) is described.

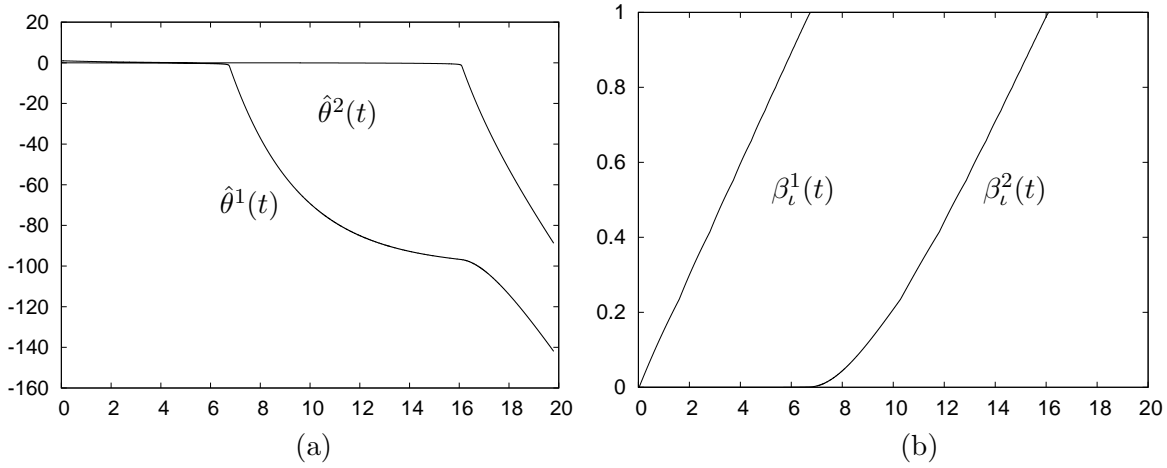


Fig 3. The case of infinite cooling rate, $\theta_{1s} = \theta_{2s}$. (a) Temperatures in the extracellular space and in the cell versus time; latent heat plateaus are present. (b) Ice fraction in the extracellular space and in the cell versus time.

Let ε be a small positive number, and t_n the current time instant. Consider the neighborhood

$$\mathcal{U}_\varepsilon = \{(x, y, z) \in \mathbb{R}^3 : |x - x(t_n)| \leq \varepsilon, |y - y(t_n)| \leq \varepsilon, |z - z(t_n)| \leq \varepsilon\}$$

of the current state $(x(t_n), y(t_n), z(t_n))$ of system (1.4). By searching through all grid points $(x_i, y_j, z_k) \in \mathcal{U}_\varepsilon$, find a point $(x_{i_*}, y_{j_*}, z_{k_*})$ such that

$$V^n(x_{i_*}, y_{j_*}, z_{k_*}) = \min_{(x_i, y_j, z_k) \in \mathcal{U}_\varepsilon} V^n(x_i, y_j, z_k).$$

The current control $u(t_n)$ which is supposed to be applied on the next time interval $[t_n, t_n + \tau]$ is computed from the condition of maximal projection of the system velocity (f_1, f_2, f_3) onto the direction of the vector $(x_{i_*} - x(t_n), y_{j_*} - y(t_n), z_{k_*} - z(t_n))$, i.e.

$$u(t_n) = \arg \max_{|u| \leq \mu} \left((x_{i_*} - x(t_n))f_1 + (y_{j_*} - y(t_n))f_2 + (z_{k_*} - z(t_n))f_3 \right).$$

It is clear that the value of the control will be either μ or $-\mu$.

6. Simulation results

Let us first consider the following two-dimensional variant of the controlled system:

$$\begin{aligned} \dot{x} &= -\alpha_1[\Theta_1(x) - \Theta_2(y)] - \lambda[\Theta_1(x) - u] - d + v_1 \\ \dot{y} &= -\alpha_2[\Theta_2(y) - \Theta_1(x)] + v_2, \end{aligned} \tag{6.1}$$

which corresponds to the assumption $z \equiv u$ (infinite cooling rate). The values of the coefficients and bounds on the control and disturbances used for all simulations are: $\alpha_1 = \alpha_2 = 0.1$, $\lambda = 2$, $d = 2$, $\mu = 4$, $\nu = 0.2$. The notation $\beta_l^i := 1 - \beta_l^i$, $i = 1, 2$, is used for the ice fractions.

We start with the case where the intra- and extracellular liquids have the same freezing points, i.e. $\theta_{1s} = \theta_{2s}$. The case of infinite cooling rate is considered (see equations (6.1)). The plots of the temperatures in the cell and pore regions versus time are given in Fig. 3a. Fig. 3b shows that the control fails to balance ice fractions in the pore and in the cell.

The next simulation (see Fig. 4) shows the case of different freezing points for the pore and the cell: $\theta_{1s} - \theta_{2s} = -13^\circ\text{C}$. Thus, the freezing point of the extracellular fluid is lowered, e.g. by adding a cryoprotector. Now, we can freeze the intracellular fluid using temperatures laying above the freezing point of the extracellular liquid, which makes simultaneous freezing possible in principle. Fig. 5 stands for the same setting but in the case of finite cooling rate (see equations (1.4)).

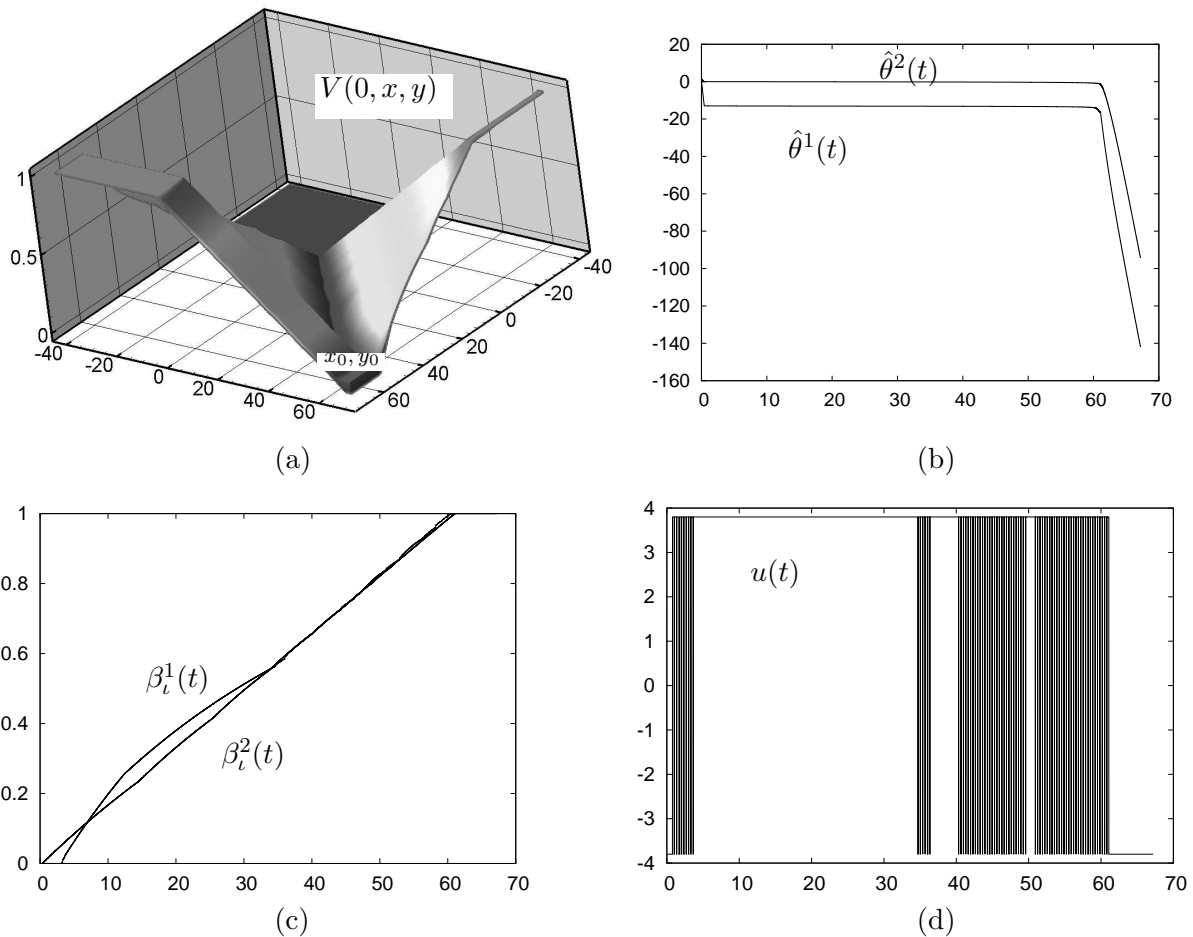


Fig 4. The case of infinite cooling rate, $\theta_{1s} - \theta_{2s} = -13^\circ\text{C}$. (a) Graph of the value function at $t = 0$. (b) Temperatures in the extracellular space and in the cell versus time; latent heat plateaus are present. (c) Ice fractions in the extracellular space and in the cell versus time. (d) Realization of the control.

7. Conclusion

A mathematical model of the intra- and extracellular ice formation proposed in the paper can be used to design optimal cooling protocols for cryopreservation of living cells. The model is formulated as a differential game in the two or three dimensional state space. The finite difference scheme proposed in [11] is applied to the computation of the value function. Numerical experiments show a very nice property of the method: the noise usually coming from the boundary of the grid region is absent. However, the numerical implementation of the method requires (especially in three-dimensional case) parallel computing. All examples presented in this paper are calculated on a Linux computer admitting 64 GB memory and 32 threads. The coefficient of the parallelization is equal to 0.9 pro thread (30 times totally). The grid size in three dimensions is 300^3 , the number of time steps is 30000 (see the restrictive relation between the space and time step sizes given by Lemma 1). The run time is approximately 20 min. In the case of two dimensions the run time is about 30 seconds. Numerical experiments show feasibility of four-dimensional computations with grids of 200^4 nodes and 5000 time steps. The run time here is not terrible (several hours), but the main difficulty consists in a tremendous data amount (terabytes) that is to process to obtain at least a picture.

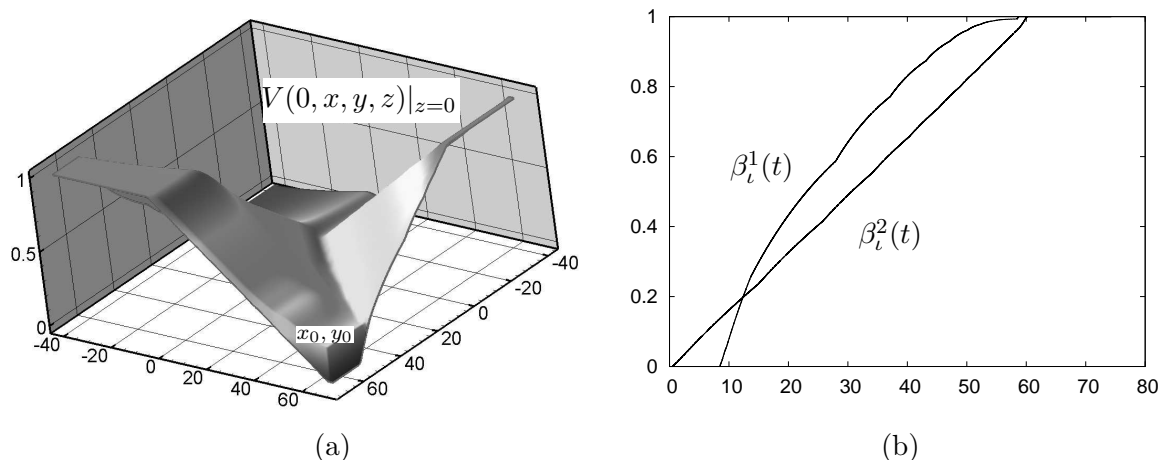


Fig 5. The realistic case of finite cooling rate (three dimensions), $\theta_{1s} - \theta_{2s} = -13^\circ\text{C}$. (a) Graph of the value function at $t = 0$, $z = 0$. (b) Ice fractions in the extracellular space and in the cell versus time.

REFERENCES

1. **Botkin N.D.** Approximation schemes for finding the value functions for differential games with non-terminal payoff functional // Analysis 1994. Vol. 14, no. 2. P. 203–220.
2. **Botkin N.D., Hoffmann K.-H., Turova V.L.** Stable Solutions of Hamilton—Jacobi Equations. Application to Control of Freezing Processes. German Research Society (DFG), Priority Program 1253: Optimization with Partial Differential Equations. Preprint-Nr. SPP1253-080 (2009). <http://www.am.uni-erlangen.de/home/spp1253/wiki/images/7/7d/Preprint-SPP1253-080.pdf>
3. **Caginalp G.** An analysis of a phase field model of a free boundary // Arch. Rat. Mech. Anal. 1986. Vol. 92. P. 205–245.
4. **Crandall M.G., Lions P.L.** Viscosity solutions of Hamilton—Jacobi equations // Trans. Amer. Math. Soc. 1983. Vol. 277. P. 1–47.
5. **Crandall M.G., Lions P.L.** Two approximations of solutions of Hamilton—Jacobi equations // Math. Comp. 1984. Vol. 43. P. 1–19.
6. **Frémond M.** Non-Smooth Thermomechanics. Berlin: Springer-Verlag, 2002. 490 p.
7. **Hoffmann K.-H., Jiang Lishang.** Optimal control of a phase field model for solidification // Numer. Funct. Anal. Optimiz. 1992. Vol. 13, no. 1,2. P. 11–27.
8. **Isaacs R.** Differential Games. New York: John Wiley, 1965. 408 p.
9. **Krasovskii N.N.** Control of a Dynamic System. Moscow: Nauka, 1985. 520 p. (in Russian).
10. **Krasovskii N.N., Subbotin A.I.** Game-Theoretical Control Problems. New York: Springer, 1988. 518 p.
11. **Malafeyev O.A., Troeva M.S.** A weak solution of Hamilton—Jacobi equation for a differential two-person zero-sum game, in: Preprints of the Eight Int. Symp. on Differential Games and Applications, Maastricht, Netherland, July 5–7, 1998, P. 366–369.
12. **Souganidis P.E.** Approximation schemes for viscosity solutions of Hamilton—Jacobi equations // J. Differ. Equ. 1985 Vol. 59. P. 1–43.
13. **Subbotin A.I., Chentsov A.G.** Optimization of Guaranteed Result in Control Problems. Moscow: Nauka, 1981. 287 p. (in Russian).
14. **Subbotin A.I.** Generalized Solutions of First Order PDEs. Boston: Birkhäuser, 1995. 312 p.

Botkin Nikolai Dmitrievich
Cand. of Phys.-Math. Sci.
Senior researcher
Tech. Universität München
Zentrum Mathematik, M6
e-mail: botkin@ma.tum.de

Hoffmann Karl-Heinz
Professor, Dr. Rer. Nat.
Tech. Universität München
Zentrum Mathematik, M6
e-mail: hoffmann@ma.tum.de

Received February 10, 2010